Supplementary Information

Multifunctional Fe$_2$O$_3$/CeO$_2$ Nanocomposites for Free Radical Scavenging Ultraviolet Protection
Dean Cardillo[a,b], Martin Weiss[a], Moeava Tehei[b,c], Thierry Devers[d], Anatoly Rosenfeld[b,c] and Konstantin Konstantinov[a]

[a] *Institute for Superconducting and Electronic Materials, Australian Institute for Innovative Materials, University of Wollongong, Squires way, Wollongong 2500*
[b] *Illawarra Health and Medical Research Institute, University of Wollongong, NSW, Australia*
[c] *Centre for Medical and Radiation Physics, University of Wollongong, NSW, Australia*
[d] *Interface, Confinement, Matériaux et Nanostructures – ICMN UMR737, Site IUT de Chartres, France*

Synthesis

For the synthesis of the composite system, Fe_2O_3 nanoparticles were resuspended and $Ce(NO_3)_3$ dissolved in DI water in separate stock solutions. These two solutions were then mixed in the desired ratios in a total of 40 mLs of DI water.

| Ce amount (at%)	Mass Fe_2O_3 (g)	Mass $Ce(NO_3)_3$ (g)
2.5	0.2	0.0272
5	0.2	0.0544
10	0.2	0.1088

Characterization

X-ray diffraction patterns were obtained using a EMMA X-ray Diffractometer (GBC Scientific Equipment), high resolution transmission electron microscopy (TEM) images were taken using a JEM-ARM200F (JEOL) atomic resolution microscope and energy-dispersive X-ray spectroscopy (EDS) mapping images obtained using a Centrino SDD 100 mm^2 detector (JEOL). A UV-3600 spectrophotometer (SHIMADZU) was used to measure the ultraviolet-visible absorption spectra of the particles. In order to investigate the free radical scavenging behaviour of the samples, a photocatalysis experiment was designed to simulate the interaction between ultraviolet light, P25 and the synthesized nanoparticles. A RPR-200 Photochemical Reactor (RAYONET) fitted with 8 x 3000 Å (21 W) and 8 x 3500 Å (24 W) ultraviolet lamps was used as a source, also featuring a cooling fan and magnetic stirrer to ensure constant temperature and homogeneity of reaction solution. These reaction solutions were comprised of 5 mg L^{-1} of P25 and 10 µmol of crystal violet (Tris(4-(dimethylamino)phenyl)methylium chloride) (Sigma Aldrich) in DI water as an indicator of free radical activity of the system, as it features a strong absorption band at 590 nm and it's carbon-carbon double bonds can be readily chemically attacked by hydroxyl radicals ($OH^{.}$), producing colourless reaction products. A total volume of 100 mLs of this dye + P25 solution was briefly sonicated before being placed in a quartz beaker (Quartz Scientific) in the photochemical reactor. After the ultraviolet lamps were switched on, 10 mL samples were taken every 5 minutes until a total of 30 minutes of irradiation had passed. These samples were then sonicated for 10 minutes, and their ultraviolet-visible absorption measured in a UV-3600 spectrophotometer (SHIMADZU) between 200-800 nm.

Results

Table S1: Energy dispersive X-ray spectroscopy quantification of Fe/Ce ratio of synthesized materials.

Sample	Fe (at%)	Ce (at%)
Fe_2O_3	99.98 ± 0.05	0.02 ± 0.04
Fe_2O_3/CeO_2 2.5 at%	99.1 ± 0.2	0.9 ± 0.2
Fe_2O_3/CeO_2 5 at%	95.5 ± 0.2	4.5 ± 0.2
Fe_2O_3/CeO_2 10 at%	89.9 ± 0.2	10.1 ± 0.2
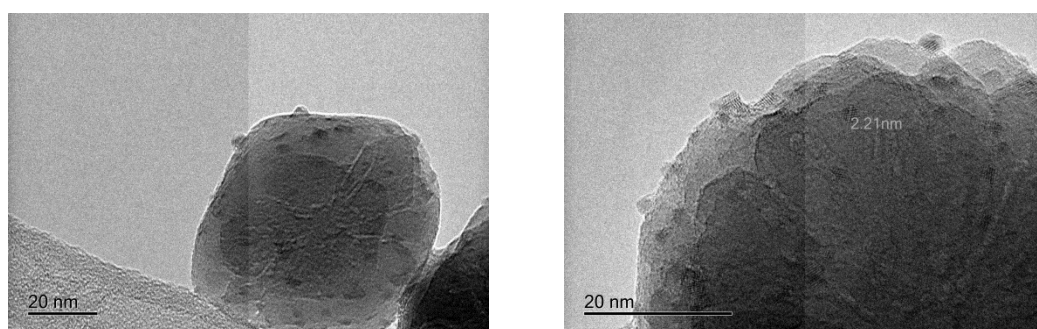
Figure S1: Transmission electron microscopy images of the Fe_2O_3/CeO_2 2.5 at% nanocomposite particles, which shows the presence of CeO_2 surface particles and their even distribution.
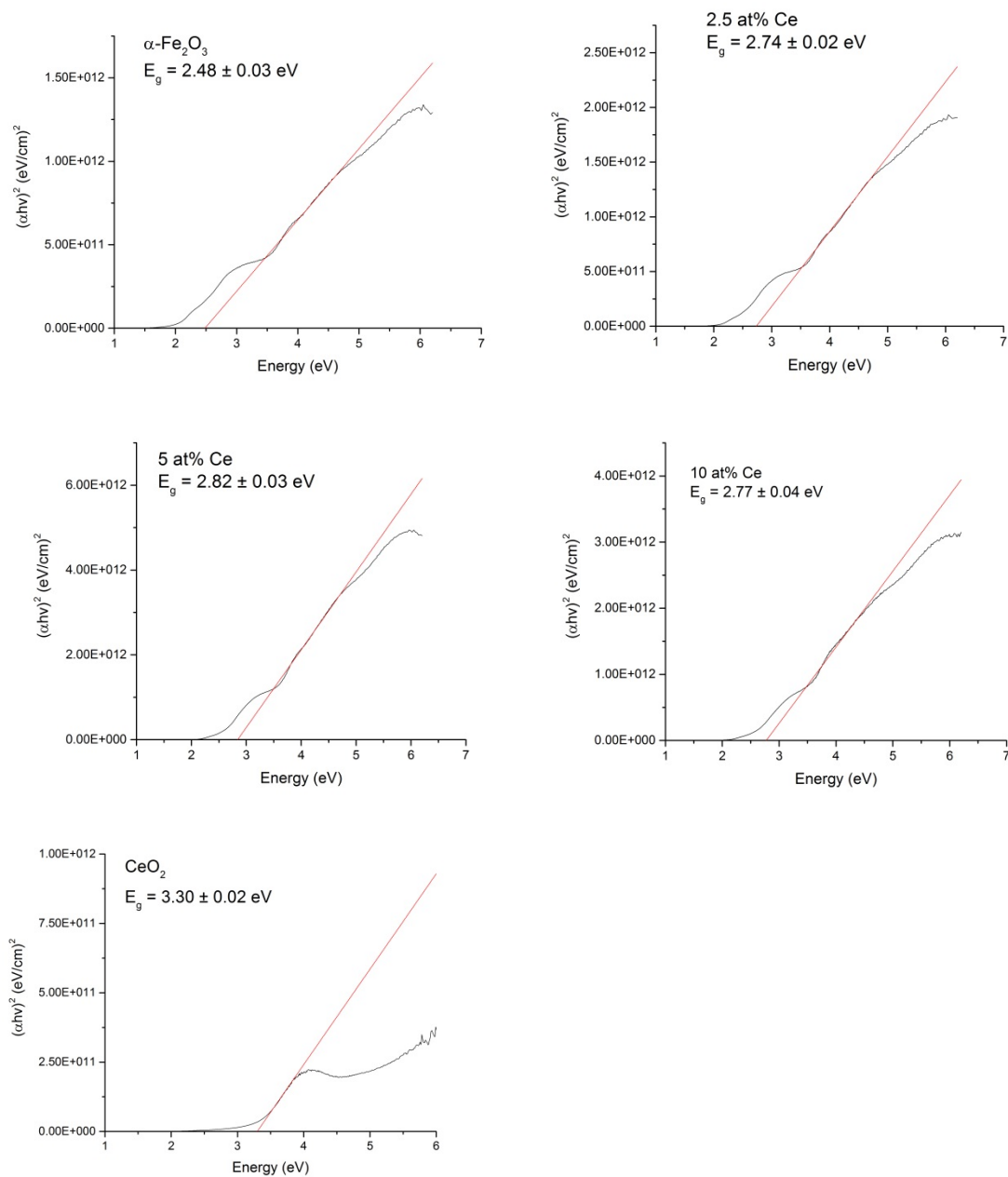
Calculation of Optical Band Gaps:

In order to calculate the optical band gap of the synthesized nanoparticles, the ultraviolet visible absorption spectra of the samples, taken at a concentration of 25 mg/L, were used to construct Tauc plots. Firstly, the following equation was used to find α:

$$\alpha = \frac{A \times \rho \times (2.303 \times 10^3)}{c}$$

Where A is the absorbance of the material at a given wavelength, ρ is the density of the material, and c is it's concentration. This α was then used to construct the Tauc plot, as a function of incoming photon energy:

$$E = (\alpha h v)^2$$

The linear portion of each curve was then fitted, and it's interception with the x-axis taken as the optical band gap energy of the nanoparticles.

Figure S2: Tauc plots for each of the synthesized nanoparticle systems, showing the optical bandgap.
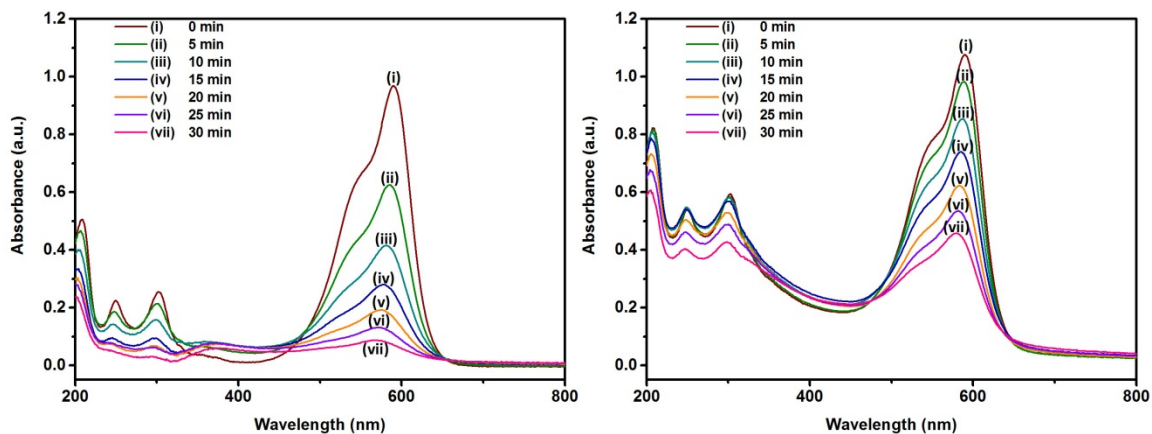
Figure S3: Degradation of crystal violet under ultraviolet light exposure in a solution of 5 mg/L of P-25 (left) and 5 mg/L of P25 and 5 mg/L of Fe_2O_3-CeO_2 (5 at% Ce) nanocomposite particles.
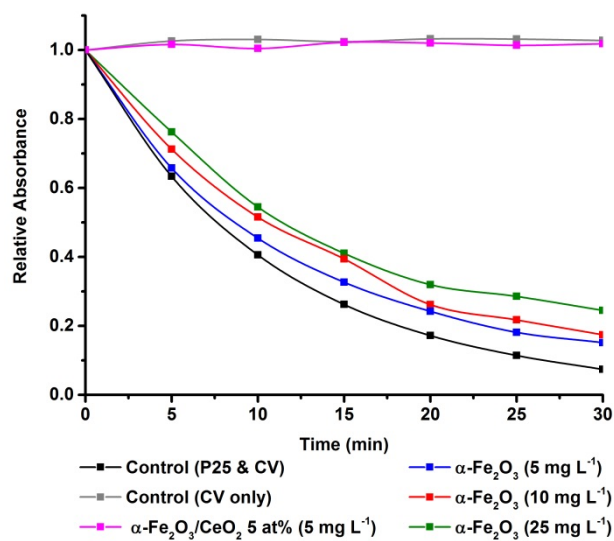
Figure S4: The influence on the addition of P-25 and hematite nanoparticles on the relative decrease in absorbance of crystal violet following difference ultraviolet light exposure times.

Table S2: Rate constants for the degradation of crystal violet (10 µmol) of various reagents when combined with P 25 in the photoreaction chamber.

Concentration of P 25 (mg L^{-1})	Reagent	Concentration of Reagent (mg L^{-1})	Rate Constant (**k**) (x 10^{-2} min^{-1})	Rate Constant Correlation Coefficient (**R^2**)
0	-	-	-0.067 ± 0.035	0.31
5	-	-	8.65 ± 0.06	0.99
5	α-Fe_2O_3	5	6.3 ± 0.3	0.99

5	α-Fe$_2$O$_3$	10	5.9 ± 0.2	0.99
5	α-Fe$_2$O$_3$	25	4.8 ± 0.6	0.97
5	α-Fe$_2$O$_3$/CeO$_2$ 2.5 at% Ce	5	5.5 ± 0.2	0.99
5	α-Fe$_2$O$_3$/CeO$_2$ 5 at% Ce	5	3.1 ± 0.1	0.99
5	α-Fe$_2$O$_3$/CeO$_2$ 10 at% Ce	5	3.3 ± 0.5	0.99
0	α-Fe$_2$O$_3$/CeO$_2$ 5 at% Ce	25	-0.046 ± 0.027	0.24
5	CeO$_2$	5	7.2 ± ra0.1	0.99

It can be seen that both experiments run without P25 did not result in any dye degradation, these experiments do not follow this experimental model, and as such, do not return good values for correlation constant R^2, or meaningful values for the rate constant **k**.

Rate constant **k** was found according to the Langmuir-Hinshelwood model, where:

$$Ln\left(\frac{C_t}{C_0}\right) = -kt$$

As such, the linear rate constant can be found by plotting **-ln(C$_t$/C$_0$)** against time, and then fitting a straight line to these points in order to find the **k.**
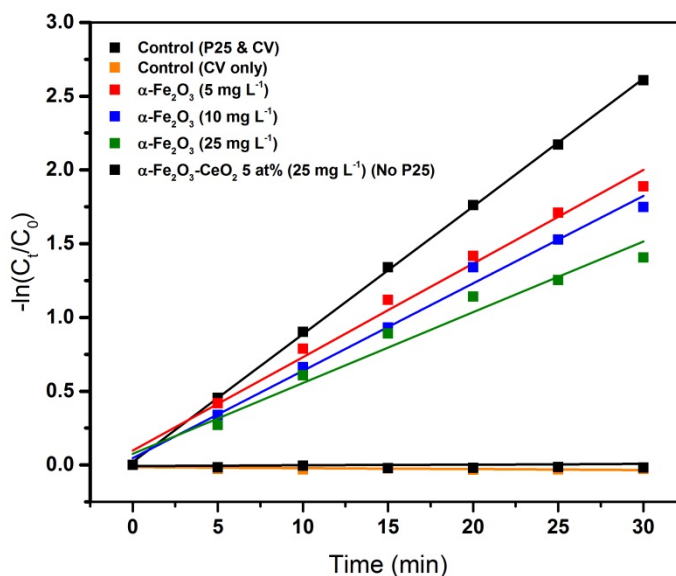
Figure S5: Linear rate constant curves for crystal violet decomposition under ultraviolet light exposure in solution with 5 mg L^{-1} P25 and synthesized nanomaterials.

**Fourier Transform Infrared Spectroscopy**

The infrared transmission spectra for each of the synthesized materials were obtained for dry powdered samples using a SHIMADZU AIM8000 FT-IR spectrometer between 500-4000 cm^{-1} and with a resolution of 8 cm^{-1}.
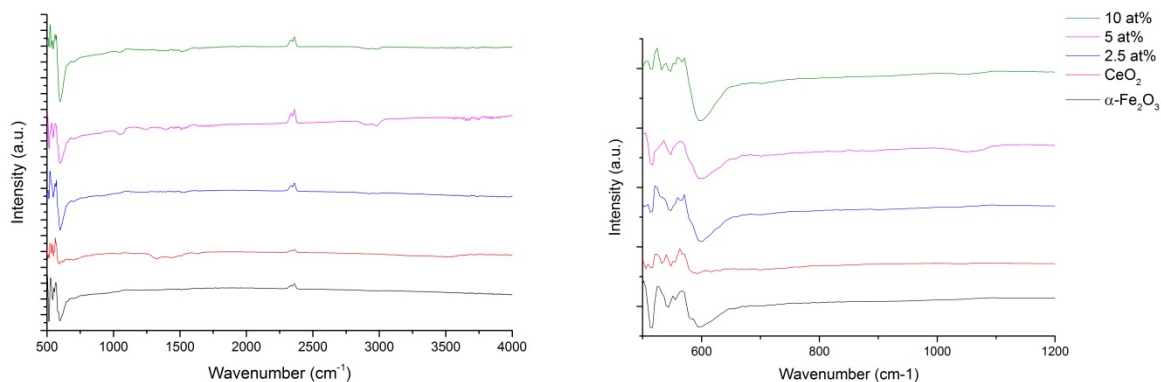
Figure S6: Fourier Transform Infrared Spectroscopy (FTIR) characterisation of the synthesised metal oxide nanoparticles and nanocomposites.

Each of the samples feature a strong peak at ~570 cm^{-1} corresponding to the $A_{2u} + E_u$ vibrational mode of hematite [1], as well as the large shoulder centered around 600 cm^{-1}. Three very weak, broad peaks corresponding to the CeO_2 phase can also be seen at 1200, 1400 and 1600 cm^{-1}. These are most visible in the pure CeO_2 and can be seen in the 5, 10 and 20 at% Ce composites [2].

Thermogravimetric Analysis
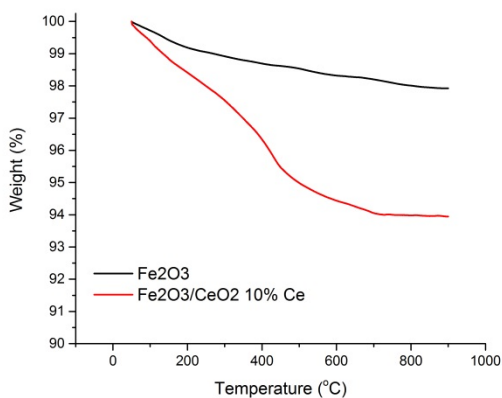
Figure S7: TGA weight loss curves for the α-Fe_2O_3 nanoparticles and 10 at% α-Fe_2O_3/CeO_2 nanocomposite particles, between 50-900 ^{o}C, at a heating rate of 10 ^{o}C/min.

The weight loss curve of the uncoated α-Fe_2O_3 nanoparticles shows a steady decrease in mass from 50-900 ^{o}C, resulting in a total mass loss of 2.1%. Given the large dislocations and cracks running along the surface of these particles, and that they were dried at 100 ^{o}C without further calcination, it is likely that this loss is due to some surface hydration, and potentially some trace unreacted precursor. The 10 at% sample shows a final weight loss of 6.1%, with an increasingly sharp loss in mass from 370-450 ^{o}C. This is likely due to some small amount of unreacted cerium nitrate present in the sample.

References:

1. A. M. Jubb and H. C. Allen, *ACS Appl. Mater. Interfaces*, 2010, 2(10) pp. 2804-2812
2. Z. Zhang, C. Hu, Y. Xiong, C. Xia, F. Li and X. Wang, *J. Wuhan Univ. Technol. Mat. Sci. Edit., 2009*, 24 pp. 34-37